DOI: 10.1002/chem.200800241

VIP

Synthesis and Optical Properties of all-*trans*-Oligodiacetylenes

Gregor S. Pilzak, Barend van Lagen, Cindy C. J. Hendrikx, Ernst J. R. Sudhölter, and Han Zuilhof*[a]

Abstract: A new series of pure and highly soluble oligodiacetylenes (ODAs) was synthesized in high yield and on a multi-milligram scale by a sequence of Sonogashira reactions with a strongly reduced level of homocoupling. The λ_{max} and ε_{max} of these ODAs show an increase with both chain elongation and solvent polarity. A plot of λ_{max} absorption versus 1/CL (CL = conjugation length) was shown to be linear. The λ_{max} converges to 435 nm for the longest members of the series at micromolar concentration. This reveals that the longest wavelength absorption observed for PDA chains (λ_{max} up to 700 nm) is due to aggregation effects. The fluorescence quantum yield increased from monomer to trimer and decreased for longer ODAs. A similar trend is found for the lifetime of fluorescence with a maximum of 600 ps for the trimer. The observed linearity of the rotational correlation time with the oligomer length implies that the ODA chains in solution lack significant geometrical changes. This implies that the ODAs in solution are fully stretched molecular rods of up to 4 nm in length.

Keywords: anisotropy · fluorescence spectroscopy · oligodiacetylenes · oligomerization · optical properties · pi interactions

Introduction

Over the last decade there has been a tremendous growth of interest in the optoelectronic properties of conducting polymers.[1,2] These polymers with linearly π-conjugated scaffolds possess unique properties such as photoconductivity and third-order nonlinear optical properties.[3–5] Most of the conjugated polymers are, however, heterogeneous in conjugation length, which hampers systematic studies of their optoelectronic properties. Moreover, the processing and characterization of these polymers can be difficult due to a low solubility in organic solvents. Therefore the dependence of the optoelectronic properties on the chain length deserves further clarification for many types of conjugated materials.[6] To obtain further insight into the consequences of extended π-conjugation, homologous series of monodisperse analogues can be investigated as a function of the chain length.[7–9] Such well-defined oligomers function as model systems to determine the evolution of the electronic, optical, thermal, and morphological properties of the corresponding polymeric materials.

Current research on the basic features of conjugated polymers is mostly devoted to the study of oligoenes,[10,11] oligothiophenes,[12–18] oligoarylenevinylenes,[19,20] oligoaryleneethynylene,[21] iso/*cis*-oligodiacetylenes (iso/*cis*-ODAs),[5,22,23] and oligotriacetylenes.[24–30] However, systematic investigations of the synthesis and optoelectronic properties of monodisperse all-*trans*-oligodiacetylenes (or *trans*-oligoenynes) still remain very scarce. This is remarkable considering that polydiacetylenes (PDAs) figure prominently in current research on electronically conducting polymers (>1500 publications since 1990[31]) and are of interest as nonlinear optical materials.[31,32] Such PDA molecular wires can act as a channel to transfer charges between sites in a molecular electronic device.[33,34] Moreover, PDAs are unique due to their formation by topochemical polymerization from crystalline diacetylenes,[35] resulting in quasi one-dimensional organic quantum wires.[31,36,37] During this process PDA chains are formed in the presence of neighboring parallel conjugated backbones. Although this may give PDAs some of their unique properties, it also blurs the distinction between intrachain and inter-chain effects. The synthesis of a systematic series of monodisperse all-*trans*-oligodiacetylenes as model

[a] G. S. Pilzak, B. van Lagen, C. C. J. Hendrikx, Prof. Dr. E. J. R. Sudhölter, Prof. Dr. H. Zuilhof
Laboratory of Organic Chemistry, Wageningen University
Dreijenplein 8, 6703 HB Wageningen (The Netherlands)
Fax: (+31) 317-484-914
E-mail: Han.Zuilhof@wur.nl

Supporting information for this article is available on the WWW under http://dx.doi.org/10.1002/chem.200800241. It contains UV/Vis data in *n*-hexane, extended comparisons of solution versus solid-state absorption spectra, and characterization data for new compounds (**1-*1*** to **1-*8***): ^{1}H and ^{13}C NMR spectra, and HRMS data.

compounds for isolated PDA chains is therefore needed to clarify this distinction, as they can be studied both in isolated form (at micromolar concentrations in solution) and with adjacent conjugated chains (in thin films of pure compound). Therefore all-*trans*-oligodiacetylenes (ODAs) can function as models for a more detailed understanding of the effects of the conjugation length on the optoelectronic properties of PDAs.

The first syntheses of ODA series ran up to penta- and heptamers,[38,39] but the low solubility of the higher analogues prevented a proper spectroscopic characterization. This was improved somewhat in the mid-1990 s, with the synthesis of a series of ODAs with *tert*-butyl endgroups that allowed a more detailed spectroscopic analysis.[40] However, *cis/trans* isomerization of oligodiacetylenes during the synthesis by means of a Peterson-olefination reaction again hampered systematic investigations.[40,41] Short *trans*-ODAs bearing phenyl and trimethylsilyl endgroups have also been synthesized as part of a π^2-complex with cobalt and molybdenum but only UV spectroscopic measurements were performed.[42]

Polhuis et al. used the Sonogashira coupling of terminal acetylenes with *trans*-1,2-dichloroethene to prepare series of ODAs ranging from monomer up to trimer with different endgroups.[43] However, the instability of terminal acetylenes, which resulted in polymerization or homocoupling reactions, prevented the formation of longer analogues. Yet, sufficient amounts of oligomer were isolated up to the trimer, to allow detailed photophysical studies of those materials.[44,45] Recently, Takayama et al. reported a synthetic approach to produce a soluble series of ODAs up to a pentamer.[46,47] The key step in this elongation method was the Sonogashira coupling of 1-iodo-4-trimethylsilylbut-1-en-3-yne with terminal acetylenes. The use of two equivalents of the halogenated diacetylene was required to partially suppress the formation of the homocoupling product of the terminal acetylenes. Nevertheless, even under these reaction conditions, 10–20% of the homocoupling product was always found in the reaction mixture along with the starting material. Although synthetically this opened the door towards further studies, the spectroscopic characterization of these ODAs was limited to NMR, IR, and UV/Vis steady-state absorption spectroscopic measurements.

In this study we present an optimized method to synthesize highly soluble ODAs **1-*n***, from monomer **1-*1*** to octamer **1-*8*** (Scheme 1) in high yields (70–80%). This allows, for the first time, the synthesis of significant amounts of these oligomers and detailed photophysical studies. Therefore, we can also report on the optical absorption and emission features of these materials by using both steady-state and picosecond time-resolved techniques, which allows discussion of a long-standing issue in the literature regarding PDAs, namely the origin of the visible light absorption of those polymers.[31]

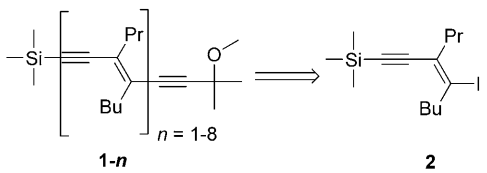

1-*n* 2

Scheme 1. Retrosynthetic approach for ODAs **1-*n*** under present study

Results and Discussion

Synthesis of all-*trans*-Oligodiacetylenes: Our approach to synthesize a series of ODAs **1-*n*** (Scheme 2) required a simple preparation of enyne **2** equipped with two different alkyl side chains. Two complementary ways to enhance the solubility and to retain the π-overlap between the subunits of the oligodiacetylenes were applied: a) *tert*-methoxy and trimethylsilyl groups at both ends of the conjugated chain, and b) short alkyl chains with different sizes on the repeating units.

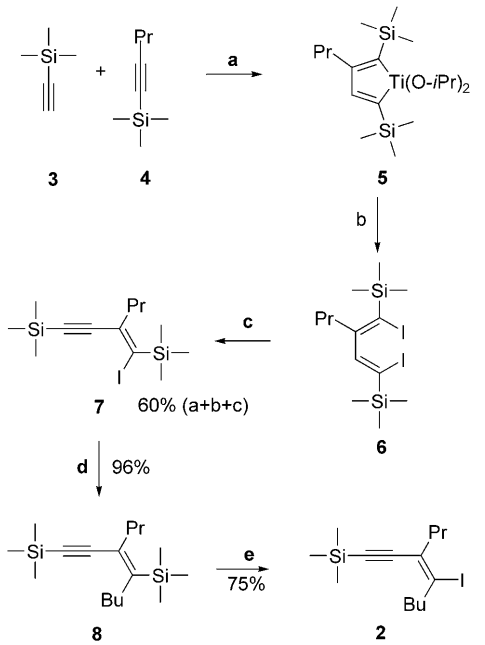

Scheme 2. Synthesis of building block **2**. Reagents: a) $Ti(OiPr)_4$, *i*PrMgCl; b) I_2; c) pyrrolidine; d) *n*BuLi, *n*BuI; e) *N*-iodosuccinimide.

The building block enyne **2** was synthesized by using the multistep method shown in Scheme 2. The regioselective coupling[48,49] between terminal acetylene **3** and internal acetylene **4** followed by iodination of titanium complex **5** and subsequent elimination of iodine was performed on a multi-gram scale to provide iododiacetylene **7** in a good overall yield (60%).[46,47] Alkylation step (Scheme 2, d) is performed by using *n*BuLi/*n*BuI to provide diacetylene **8** in excellent yield (96%). We found that the use of the *n*BuLi reagent instead of a tertiary lithium salt[46] improved the yield of the desired product oligodiacetylenes by in situ formation of the alkylating reagent, *n*-butyl iodide.[50] The for-

mation of this compound close to the reaction site speeds up the conversion, and prevents the occurrence of otherwise-competing reactions. As a result, the formation of a protonated analogue of **7** is completely suppressed, however, this is not the case when *t*BuLi and *n*BuI are used.[51] Moreover, other commercially available or easily prepared organolithium salts may be utilized for this alkylation step, which provides a general route to variation in the side chain length. For example, we used *n*-heptyllithium and *n*-heptyl bromide to prepare diacetylene **8a** with *trans*-propyl and heptyl side chains in nearly identical yields (Scheme 3), but since further development of this synthesis was beyond the scope of this study we have consistently used building block **2**. The iodination step is performed with *N*-iodosuccinimide, which provides enyne **2**. The final purification of this apolar compound requires the use of reversed-phase silica material to remove any traces of the side products.

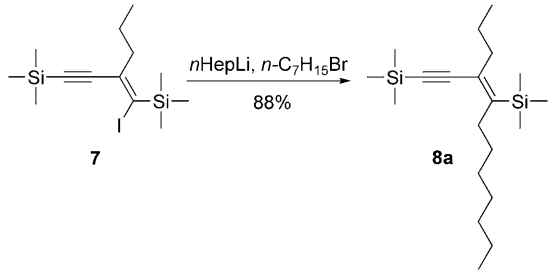

Scheme 3. Alkylation of iododiacetylene **7** with *n*-heptyllithium.

Enyne **2** is catalytically coupled with 2-methylbut-3-yn-2-ol by a Sonogashira coupling,[52] which results in the formation of enediyne **9** bearing two different endgroups (Scheme 4). To increase the stability of the radical cations of these conjugated materials (studies to be published elsewhere)[53] the tertiary hydroxy endgroup was transformed into the redox-insensitive methoxy group. Direct methylation of hydroxy *trans*-oligodiacetylenes with NaH and MeI resulted in the almost quantitative formation of methoxy analogues. These were subsequently subjected to protodesilylation in an alkaline environment (Scheme 4). The difference in reactivity against, for example, nucleophilic attack between these two endcaps made it possible to remove selectively only the TMS group to prepare a terminal acetylene (**10-*n***), which could be subjected to the following chain-elongation step by an iterative coupling with building block **2.** Moreover, the choice of the polar, methoxy-containing endcap is highly useful as it increases the polarity of the ODAs and longer analogues and allows easy purification.

The iterative elongation steps of the ODA chain, such as the formation of dimers and trimers, are subsequently achieved by using the Sonogashira coupling reactions, and have been optimized in our laboratory to achieve very good overall yields and suppression of the formation of the main side product. It is known that the use of copper(I) salts as co-catalysts in the Sonogashira coupling promotes the formation

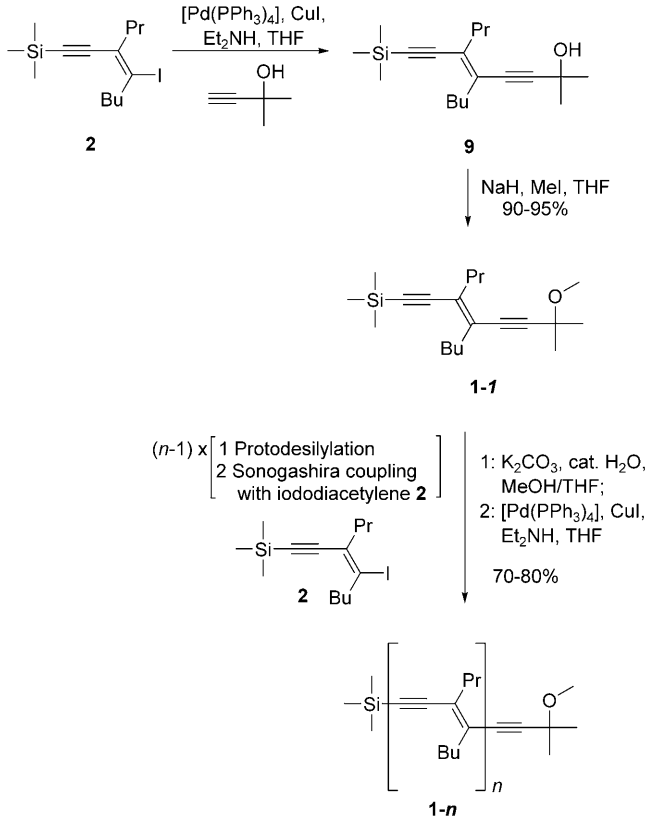

Scheme 4. Iterative synthesis of all-*trans*-oligodiacetylenes through Sonogashira coupling.

of homocoupled ODA analogues **11-*n*** (Scheme 5).[43,46,47] This copper-catalyzed oxidative homocoupling reaction has been widely applied in the synthesis of bisacetylenes.[54] However, the homocoupling is very undesirable for ODA synthesis because it consumes the terminal acetylene and reduces the yield of cross-coupled product dramatically. We succeeded in suppressing this homocoupling to about 5 mol% by the use of a large excess of **2**, up to 10 equivalents,

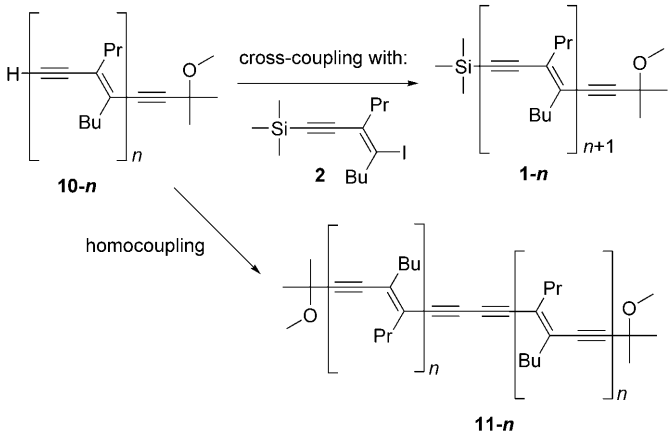

Scheme 5. Catalytic coupling of ODAs under Sonogashira conditions yielding cross-coupled and homocoupled ODAs. Reagents: $[Pd(PPh_3)_4]$, CuI, Et_2NH, THF.

under a reductive atmosphere of a 1:1 mixture of H_2/Ar. In this reaction, iodoenyne **2** was recovered quantitatively after each elongation step, which allowed the use of this large excess. A similar procedure for the Sonogashira coupling, which used a diluted atmosphere of hydrogen gas was recently published by Elangoven et al.[55] Other methods, such as the copper-free Sonogashira coupling published by Urgaonkar et al.[56] proved to be unsuitable for the synthesis of *trans*-oligodiacetylenes bearing TMS endgroups, as the instability of the TMS group against attack from a nucleophilic base such as tetrabutylammonium acetate resulted in polymerization of the ODAs.

Steady-state optical absorption in solution: The excellent solubility of the synthesized ODAs, which is largely a consequence of the laterally appended alkyl chains, allowed us to make an extended study of their optical properties. The ground-state absorption of the **1-*n*** series was measured in solution and as a drop-casted thin film. The absorption of the ODA series **1-*n*** up to the octamer as a monodisperse solution in 1,2-dichloroethane (DCE) is depicted in Figure 1. Similar spectra were obtained in *n*-hexane and are given in the Supporting Information.

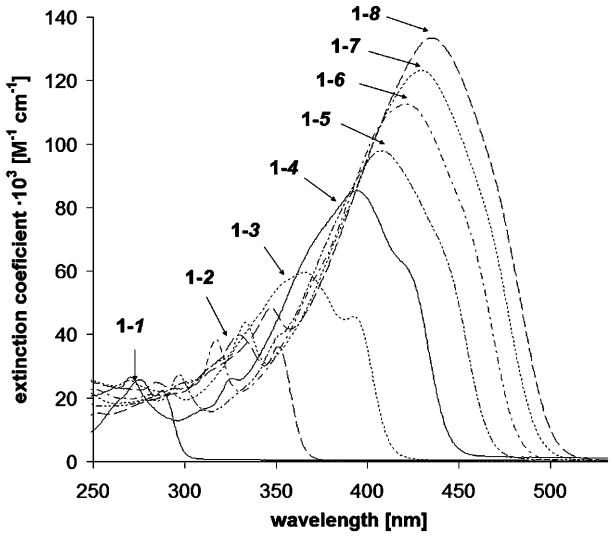

Figure 1. Electronic absorption spectra of methoxy-endcapped oligodiacetylenes **1-*n*** (***n*** = 1–8) in DCE.

The C_{2h} symmetry of the conjugated system of the ODAs under study implies that the absorption spectrum is associated with the S_2 (1^1B_u) ← S_0 (1^1A_g) transition.[44,45,57] The steady-state absorption spectra recorded in both solvents show the expected redshift of the maximum absorption peak (λ_{max}) and an increase of the extinction coefficient (ε_{max}) with an increasing number of repeating enynic units analogous to literature data reported for shorter diacetylene-based series.[38,40,44,46] The longest-wavelength absorption maximum shows that this bathochromic shift decreases significantly for the longer oligomers: $\Delta\lambda_{max}$ decreases from about 0.75 eV going from **1-*1*** to **1-*2*** to about 0.05 eV from **1-*7*** to **1-*8*** in both *n*-hexane and DCE. The solvent effect on the shift of the electronic absorption is small for this series of ODAs and is in agreement with previously reported data for shorter all-*trans*-[31,44] and *iso*-PDA oligomers.[58] For example, upon changing the solvent from *n*-hexane to DCE the longest-wavelength absorption maximum for ODAs increases from 0.02 eV (1 nm) for monomer **1-*1*** to 0.05 eV (8 nm) for octamer **1-*8*** (Table 1). This indicates that the dipole moment μ of the excited state of ODAs is only somewhat larger than that of the ground state.

Table 1. Absorption data of methoxy-endcapped oligodiacetylenes **1-*n*** (***n*** = 1–8) in *n*-hexane and DCE .

1-*n* (CL)[a]	λ_{max} [nm] ([eV])		ε_{max} [$\times 10^3$ dm^3 mol^{-1} cm^{-1}]	
	n-hexane	DCE	*n*-hexane	DCE
1–*1* (3)	274 (4.53)	275 (4.51)	24.0	25.8
1–*2* (5)	327 (3.79)	330 (3.76)	33.4	39.9
1–*3* (7)	361 (3.43)	366 (3.39)	45.7	59.6
1–*4* (9)	388 (3.20)	395 (3.14)	51.9	85.3
1–*5* (11)	401 (3.09)	410 (3.02)	63.1	100.5
1–*6* (13)	414 (3.00)	422 (2.94)	72.7	112.6
1–*7* (15)	422 (2.94)	430 (2.89)	85.5	123.2
1–*8* (17)	427 (2.90)	435 (2.85)	99.7	133.4

[a] Conjugation length (CL) = number of double/triple bonds.

The extinction coefficient is also slightly affected by the solvent polarity and this solvent effect depends on the number of enynic units as well. For the shorter ODAs the difference between ε_{max} in *n*-hexane and DCE is marginal (7.5 % in favor of the polar solvent for **1-*1***), but this increases for the longer oligomers, up to 64 %. Clearly, the $S_2 \rightarrow S_0$ transition is more probable in polarisable DCE than in *n*-hexane. It is also known that for conjugated polyenes[59] the S_2 energy level decreases with solvent refractive index (n), and this tendency is displayed for the series of ODAs, which show lower values in DCE ($n = 1.445$) than in *n*-hexane ($n = 1.375$).

The absorption maximum of the oligomers (expressed in energy units) displays a linear relation to the reciprocal number of conjugation length (1/CL) with $CL = 2n + 1$ as shown in Figure 2. An extrapolated λ_{max} of 2.55 eV (487 nm) is obtained for a polymer with $n = 8$ in *n*-hexane, whereas in DCE a value of 2.48 eV (500 nm) was measured. The absorption maximum of the longest ODA (**1-*8***) in solution is 427 and 435 nm in *n*-hexane and DCE, respectively, and the absorption spectrum of the ODA series does not exceed 500 nm for any of the compounds (see Figure 1). For plots like these, it is known that for extended oligomers they start to deviate from linearity, and curve horizontally.[60,61] In other words: based on the data that can be provided up to the octamer **1-*8***, it can be expected that the isolated polymer should display its maximum absorption at energies larger than 2.5 eV (≈500 nm). From this observation we conclude that the reported longer wavelength absorptions (λ_{max} up to 700 nm) for PDA chains[31] are due to aggregation effects. Such aggregation generally plays a role in con-

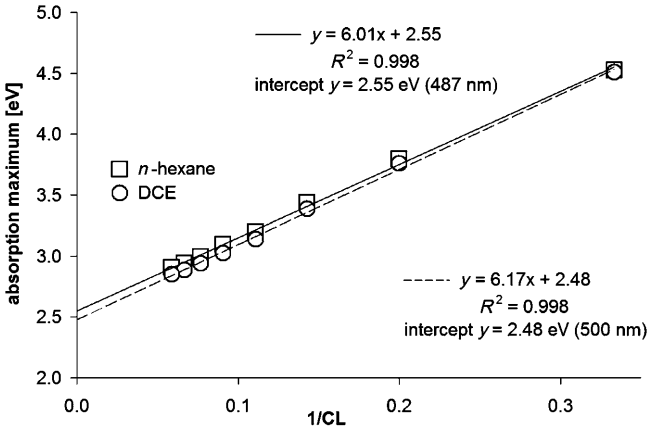

Figure 2. λ_{max} of the absorption of ODA series **1-*n*** (***n*** = 1–8) in *n*-hexane (□) and DCE (○) solution at micromolar concentrations (2×10^{-6} M) versus 1/CL.

jugated polymers, but is in our case negligible for these oligomers in dilute solution. Also at higher concentrations, up to 5 mM, ODA solutions do not show any additional high-wavelength absorption to suggest aggregation in solution. This was also the case when small amounts of methanol or ethanol were added: up to the point that a stepwise increase in the alcohol concentration starts to induce precipitation of the ODAs, no long-wavelength band could be observed in the UV/Vis absorption spectrum. This indicates that steric repulsion from the alkyl chains remains dominant for ODAs in solution.

It is important to point out that the linear relationship of the absorption maximum with 1/CL indicates that for the longer ODAs elongation of the conjugation length is observed (the curve does not yet flatten towards the *y* axis). As a result, for these oligomers with up to 17 conjugated double and triple bonds, the effective conjugation length (ECL), in which the delocalization is predominantly present in only part of the chain, is at least 17 and most likely >20. This is in contrast with the estimated ECL of 12 for PDA by Wenz et al.,[62] and more in line with predictions of Giesa and Schulz,[40] who suggest that saturation should not occur below CL = 20. In the present case, conjugation is not significantly reduced by kinks or torsions in the oligomeric chains, which shows the importance of detailed studies of extensive series of well-defined conjugated oligomers. Analogous data presented for polytriacetylenes by Martin et al. show truncation effects for that type of oligomer only with more than 24 conjugated bonds.[63] Finally, a recent study of oligoenes with up to 15 conjugated C=C bonds by Czeakalius et al.[11] is also in good agreement with the presented linear correlation of λ_{max}, the absorption maximum with 1/CL.

Steady-state optical absorption in thin films: The optical absorption of the ODA series in the solid state was investigated in drop-casted thin films. The absorption spectrum was taken 30 min after the evaporation of the solvent, and for **1-*8*** also after 12, 24, and 48 h. Because the shorter oligomers up to *n* = 3 are liquids, we prepared a trimer **1-*3* OH** having a $-C(CH_3)_2CH_2OH$ endcap rather than a $-C(CH_3)_2CH_2OCH_3$ endcap by a similar approach to that shown in Scheme 4. This oligomer is a solid at room temperature, thus readily allowing absorption measurements of its drop-casted thin films. The absorption spectra are shown in Figure 3 for all solid-state ODAs. A comparison between solution and thin-film absorption is depicted in Figure 4 for **1-*3*** and **1-*8***; other oligomers show similar effects and their absorption data are part of the Supporting Information.

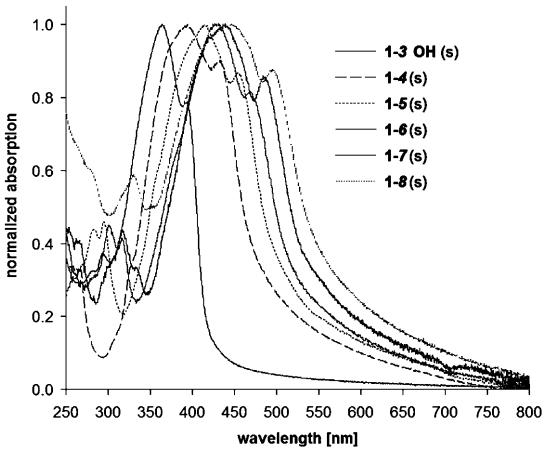

Figure 3. Normalized absorption spectra of drop-casted thin films of methoxy end-capped ODAs **1-*4*** to **1-*8***, and hydroxy end-capped ODA **1-*3* OH** taken after 12 h.

The solid-state absorption spectra of the oligomers under study consistently show two features that more or less deviate from the data in solution (see Table 2). First, additional higher-wavelength absorption occurs. Second, a clearly visible redshifted shoulder occurs that is already present for shorter oligomers in solution, but not for longer oligomers. The long-wavelength absorption feature is already detectable for the solid −OH end-capped **1-*3* OH**, in contrast to the liquid $-OCH_3$ end-capped **1-*3*** (Figure 4, top). Because the end-cap modification has no significant effects on the π system and thus on the nature of the electronic transitions, any differences between the absorption spectra of **1-*3* OH** and **1-*3*** are due to differences in the phase (solid or liquid). We attribute this solid-state effect to forced aggregation of the chains, which induces the overlap of π–π orbitals and the redshift of the λ_{max}. In other words: the absorption at >425 nm is due to solid-state effects. (The increase in the absorption of the left shoulder in the spectrum is attributed to light scattering.) This effect leads to substantial long-wavelength absorption for longer oligomers as well, and for **1-*8*** for example, the absorption at >550 nm is clearly not due to properties of isolated oligomer chains. It should be noted that this long-wavelength absorption feature (absorption at >550 nm) does not occur in concentrated solutions

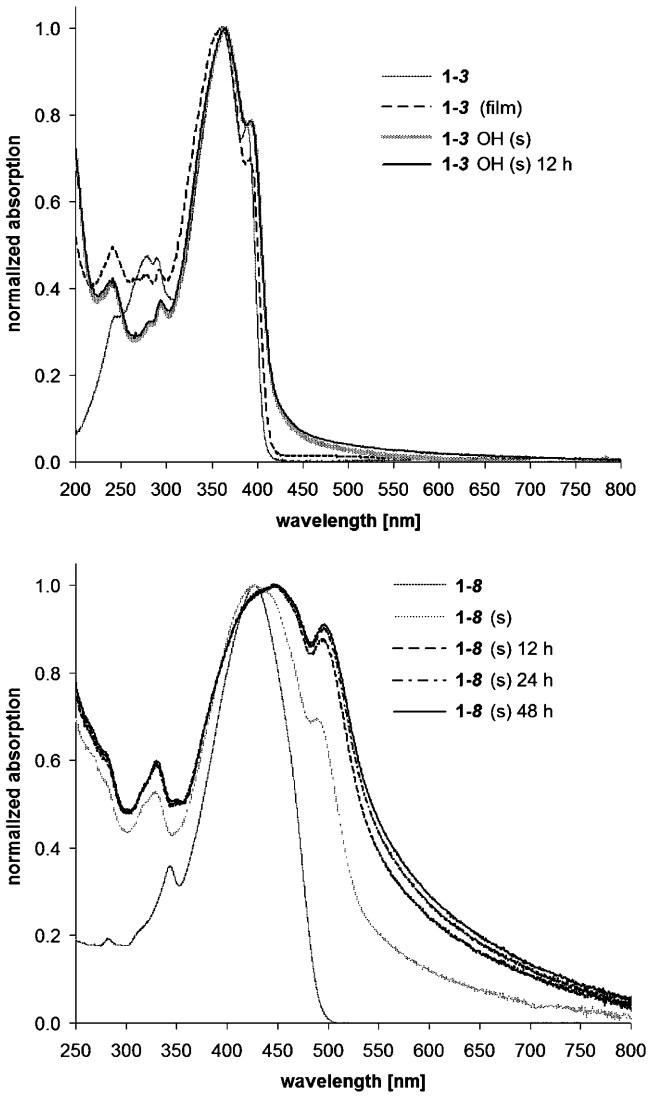

Figure 4. Normalized absorption spectra of ODAs **1-*3*, 1-*3* OH** (top) and **1-*8*** (bottom) in *n*-hexane versus solid state (s).

Table 2. Solid-state absorption data of methoxy-endcapped oligodiacetylenes **1-*n*** ($n=4$–8) and **1-*3* OH** with a *tert*-OH endcap.

1-*n* (CL)[a]	λ_{max} [nm] ([eV])	$\lambda_{max\ right\ shoulder}$ [nm] ([eV])
1-*3* OH (7)	363 (3.42)	392 (3.16)
1-*4* (9)	392 (3.16)	431 (2.88)
1-*5* (11)	413 (3.00)	452 (2.74)
1-*6* (13)	425 (2.92)	467 (2.66)
1-*7* (15)	438 (2.83)	483 (2.57)
1-*8* (17)	445 (2.79)	495 (2.51)

[a] Conjugation length (CL) = number of double/triple bonds.

(up to 5 mM), indicating that the lateral alkyl chains provide sufficient repulsion to prevent aggregation of the ODAs.

For longer oligomers, such as **1-*8***, the absorption spectrum displays no features in solution, but in the solid-phase a shoulder appears, which is already present for shorter oligomers, such **1-*3***, in both phases (liquid or solid). We interpret this to mean that for short oligomers, the completely flat oligomer geometry (C_{2h}-like) is dominant, as was confirmed from detailed photophysical studies.[44,45] For longer oligomers, entropic reasons might also allow other geometries to play a role (e.g. with slight rotations around the C–C bonds), and the lowest energy transition may even be fully suppressed in solution for these reasons. In the solid state, interchain interactions may force planarity, and thus bring back the shoulder.

For long oligomers, such as **1-*8***, an additional 20 nm redshift of λ_{max} in the spectrum is detected after 12 h, together with a significantly increased long-wavelength absorption (>550 nm for **1-*8***). We assign this to increased π–π stacking, for which there is apparently sufficient driving force; even though the process is relatively slow (time scale of several hours) due to the restrictions of the solid phase, and/or slow evaporation of trace remnants of the solvent. No marked changes in the spectra occur after 24 or 48 h, which indicates that the stacking process for these materials is largely finished within 12 h. Similar irreversible chromatic changes have also been observed for a variety of PDAs.[31] For the first time this systematic study of the optical properties of this series of oligomers thus enables us to clearly distinguish intra- and intermolecular effects on the light absorption of elongated enynic systems.

Steady-state fluorescence in solution: Emission spectra measured for near-equimolar (2×10^{-6} M) homogeneous solutions of ODA series were recorded in *n*-hexane and DCE. The emission spectra recorded in DCE are shown in Figure 5. This plot shows a redshift of λ_{max} with an increasing chain length *n*, whereas a maximum fluorescence quantum yield (Φ_f) is observed for the trimer ($\Phi_f=0.325$; see Table 3); both shorter and longer oligomers display less fluorescence. The obtained quantum yields for the methoxy-endcapped ODAs up to the trimer are similar to those previously reported for analogous ODAs of similar length.[44] Upon fur-

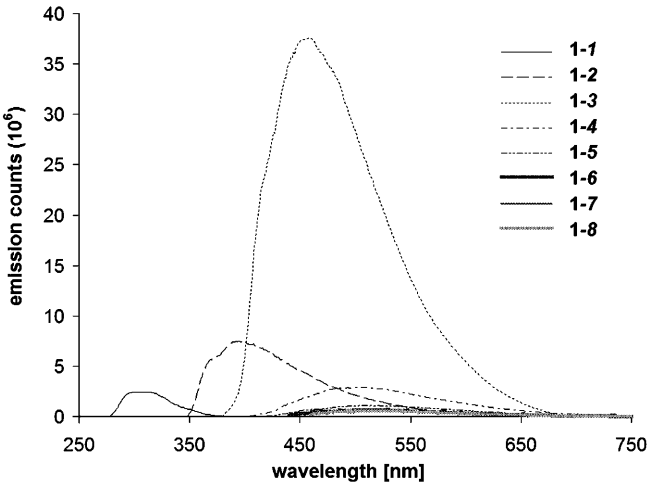

Figure 5. Fluorescence spectra of methoxy-endcapped oligodiacetylenes **1-*n*** ($n=1$–8) in DCE.

Table 3. Emission data of methoxy-endcapped oligodiacetylenes **1-*n*** (***n*** = *1–8*) in DCE and *n*-hexane.

1-*n*	Emission λ_{max} [nm] ([eV])		Quantum Yield Φ_f [a,b]	
	n-hexane	DCE	*n*-hexane	DCE
1–*1*	307 (4.04)	309 (4.01)	0.004	0.009
1-*2*	404 (3.07)	395 (3.14)	0.029	0.057
1-*3*	471 (2.63)	457 (2.71)	0.159	0.325
1-*4*	515 (2.41)	510 (2.43)	0.015	0.029
1-*5*	515 (2.41)	515 (2.41)	0.004	0.011
1-*6*	[c]	516 (2.40)	[c]	0.011
1-*7*	[c]	518 (2.39)	[c]	0.008
1-*8*	[c]	520 (2.38)	[c]	0.008

[a] Quantum yield determined by comparison with quinine bisulfate in 0.1 M H_2SO_4: $\Phi_f = 0.535$[69]. [b] Experimental error ± 0.002. [c] Not available due to marginal emission.

ther extension of the conjugation the Φ_f becomes smaller again. These values are in line with reported PDA polymer data, which show marginal fluorescence quantum yields, mostly lower than 0.001.[31,64] This can be explained by considering the electronic states involved in the light absorption process and subsequent relaxation: after excitation to S_2 (1^1B_u) (excitation to S_1 (1^1A_g) is symmetry forbidden),[44,65] rapid internal conversion takes place to the S_1 state with a time constant of about 200 fs for trimer ODA.[45] This value matches rather closely with the lifetime of the photoexcited 1^1B_u exciton in blue-phase PDAs, which was concluded to relax to the 2^1A_g exciton.[31,66] As a result, efficient population of the S_1 state through the S_2 state is expected, irrespective of conjugation length. The marked dependence of Φ_f is therefore related to a faster internal conversion from S_1 to S_0 for longer ODAs, because longer conjugated chains provide an increasing density of states, which promotes internal conversion. Similar correlations have been found for series of polyenes.[67,68] However for larger ODAs the symmetry restriction to C_{2h} might be less strict than for shorter ones due to increased conformational freedom, the increase of the rate for internal conversion will be likely to be substantially larger. The overall result is thus the remarkable decrease of the fluorescence quantum yield.

The fluorescence quantum yield recorded for the tetramer **1-*4*** up to the octamer **1-*8*** decreases more rapidly in *n*-hexane than in the more polar solvent DCE, with the emission recorded in DCE on average more than twice as high as in *n*-hexane. The 0–0 transition is only clearly visible for the emission of dimer **1-*2***. The shoulder at the high energy side of the fluorescence band is less visible for trimer **1-*3*** and cannot be resolved for monomer and longer ODAs with more than three monomeric units. With the present data it is therefore not possible to study the evolution of the Stokes shift with increasing conjugation length. This would have been interesting given the significant Stokes shifts of the smaller ODAs.[44]

Fluorescence lifetimes and anisotropy: Picosecond time-resolved single photon counting at four different excitation wavelengths (283, 304, 372, and 444 nm) was used to determine the fluorescence lifetimes of the oligomeric series **1-*n***. The observed lifetimes in the ODA series measured in *n*-hexane and DCE are listed in Table 4. The decay curves can be fitted with a sum of two exponentials. The data in

Table 4. The rotation correlation time τ_R of **1-*n*** (***n*** = *1–8*).

1-*n* (CL)[a]	τ_R [ps]	
	n-hexane	DCE
1–*1* (3)	65[b]	95[b]
1-*2* (5)	106[b]	180[b]
1-*3* (7)	155	321
1-*4* (9)	204	395
1-*5* (11)	263	468
1-*6* (13)	[c]	540
1-7 (15)	[c]	577
1-*8*(17)	[c]	631

[a] Conjugation length. [b] Values are relatively inaccurate due to low emission. [c] Not available due to marginal emission.

Table 4 indicate that the excited-state lifetimes of oligomers are positively affected by the solvent polarity: in DCE the lifetimes are generally longer than in *n*-hexane. Moreover, the longest lifetime, in both solvents, is recorded for trimer **1-*3***. The average fluorescence lifetime τ_{AVG} was calculated according to:

$$\tau_{AVG} = \frac{A_1}{A_1 + A_2}\tau_1 + \frac{A_2}{A_1 + A_2}\tau \quad (1)$$

where A_1 and A_2 are the contributions of the decays obtained from the curve fitting. The average lifetimes are <60 ps for monomer and dimer, with a maximum around 600 ps for the trimer. For oligomers longer than three enynic units the lifetime τ_{AVG} in DCE decreases from 145 ps, recorded for **1-*4***, to 25 ps for **1-*8***. In *n*-hexane a similar trend is found, analogous to the trends shown for the fluorescence quantum yields of the ODAs in Table 4.

Fluorescence depolarization (r) of the ODAs herein was studied by picosecond time-resolved fluorescence anisotropy measurements.[70] This technique can provide information regarding the transition dipole moment and molecular geometry, and has proven to be useful in recent investigations of the conformational behavior of (water)-soluble polymers in solution.[71,72] Since all-*trans* ODAs are roughly rod-shaped in their most extended conformation, and possess a relatively large axial ratio, the rotation of the molecules around the longitudinal axis progresses evidently much faster than the rotations around the two short, perpendicular axes, which are not expected to differ significantly from each other. In line with this, the observed anisotropy decay kinetics $r(t)$ of ODAs are mono-exponential, characterized by an initial anisotropy value r_0 and one rotation correlation time (τ_R):[69]

$$f(t) = r_0 \times \exp(-t/\tau_R) \quad (2)$$

in which r_0 is determined by the angle γ between the absorption and emission transition moment:

$$r_0 = \frac{(3\cos^2\gamma - 1)}{5} \quad (3)$$

The recorded initial anisotropy value r_0 for all ODAs under study was about 0.3, similar to that of trimeric ODAs investigated previously.[31,44,45] This indicates a small angle (≈15°) between absorption and emission transition moments.

The rotation correlation times of anisotropy τ_R for ODAs recorded in *n*-hexane and DCE are listed in Table 5 for those oligomers with sufficient fluorescence to determine this (to **1-*5*** in *n*-hexane and to **1-*8*** in DCE).

Table 5. Fluorescence lifetimes τ_F (in ps), their relative weights A, and average lifetimes τ_{AVG} (in ps).

1-*n* (CL)[a]	*n*-hexane			DCE		
	τ_1 (%A_1)	τ_2 (%A_2)	τ_{AVG}[b]	τ_1 (%A_1)	τ_2 (%A_2)	τ_{AVG}[b]
1-*1* (3)	24[c] (100)			24[c] (98)	647 (2)	37
1-*2* (5)	29[c] (98)	843 (2)	45	47[c] (99)	850 (1)	55
1-*3* (7)	278 (14)	647 (87)	596	237 (14)	663 (86)	603
1-*4* (9)	76 (93)	697 (7)	120	67 (83)	523 (17)	145
1-*5* (11)	15 (93)	563 (7)	53	31 (85)	678 (15)	128
1-*6* (13)	[d]	[d]	[d]	21 (96)	288 (4)	32
1-*7* (15)	[d]	[d]	[d]	24 (98)	284 (2)	29
1-*8* (17)	[d]	[d]	[d]	20 (98)	250 (2)	25

[a] Conjugation length. [b] Calculated by using Equation (1). [c] Values not accurate, as instrument response time is 560 and 460 ps, respectively. [d] Not available due to marginal emission.

The anisotropy lifetimes increase with the oligomer length, which means that the rotation time around the perpendicular axis increases for longer oligomers. The overall trend is illustrated in Figure 6, and shows a linear dependence for τ_R and the length of the fully stretched oligomer. Such linearity has recently also been observed for conformationally rigid species of similar sizes.[73] Under simplified conditions,[72] $\tau_R = \eta V/RT$, and the molecular volume $V \approx lr^2$, in which η = viscosity, l = length of the molecule, and r = molecular diameter. In other words: τ_R should be proportional to the length of the molecule. Since the observed linear correlation is with the length of the molecule in its fully extended shape, this provides clear evidence that there are no significant geometrical changes of ODA structures within this series. In other words: ODA oligomers in solution are indeed largely fully stretched nm-sized molecular rods.

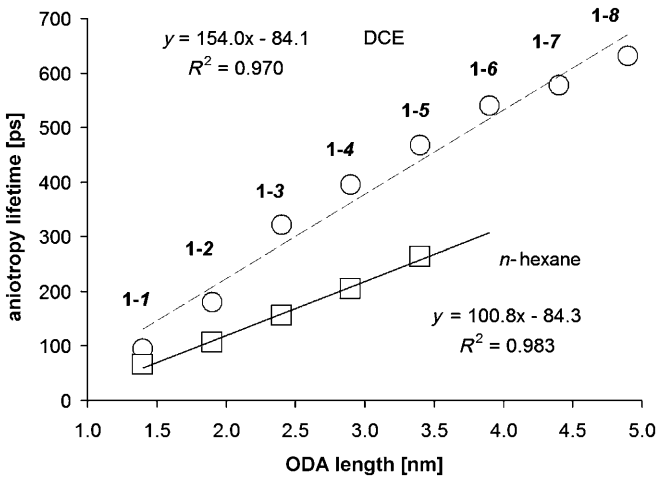

Figure 6. Anisotropy lifetimes versus the length of a fully stretched ODA molecule for **1-*1*** to **1-*8*** in DCE (○), and for **1-*1*** to **1-*5*** in *n*-hexane (□).

Conclusion

A Sonogashira reaction-based synthesis of a series of highly soluble oligodiacetylenes (ODAs) was developed, with both high yields in the chain elongation step (70–80%) and high purity (>99%). The series ranges from monomers to octamers, which contain up to 17 double and triple bonds (≈3.9 nm) and have different endcaps and alkyl side chains. The oxidative homocoupling of terminal acetylenes, which is an undesirable side reaction, has been strongly reduced by the use of an H_2/Ar atmosphere, which improves the yield of the main product significantly.

Two effects were observed for the $S_2 \leftarrow S_0$ transition of ODAs:

1) The linearity of the plot of λ_{max} versus 1/CL (conjugation length (CL) = number of double/triple bonds) displays the undiminished elongation of the conjugation length for oligomers up to 3.9 nm;
2) Solid-state absorption measurements display an additional band in the visible region. This extra band is attributed to intermolecular π–π stacking, which is marginal for oligomers at micromolar concentrations (λ_{max} = 435 nm for all ODAs), but apparently dominant in PDAs for which λ_{max} up to 700 nm have been observed.

The rotation correlation time of the anisotropy increases linearly with the oligomer length, which shows that the oligomers lack significant geometrical changes and kinks in their conjugation. This provides evidence that the ODA oligomers in solution are indeed fully stretched molecular rods.

Experimental Section

Solvents and reagents: For all dry reactions performed under a steady stream of argon (or reductive atmosphere of argon/hydrogen mixture 1:1), the equipment was dried in an oven at 150 °C for several hours and allowed to cool down in an atmosphere of dry nitrogen or argon. Pure, dry, and degassed ether and THF were obtained by distillation of the commercial material over sodium particles. CH_2Cl_2 was distilled and dried over calcium hydride or sodium hydride. Dry DMF was purchased from Sigma-Aldrich and stored under argon. All other specified chemicals were commercially purchased (Aldrich, Fluka or Riedel-de Haën) and used without further purification.

General workup and purification procedure: Reaction monitoring and reagent visualization were performed on silica gel or reversed-phase silica gel plates with UV-light (254 and 366 nm) combined with GC/MS. Usually the reaction mixture was diluted with water and extracted (3×) with

an organic solvent (petroleum ether 40–60, hexane, or ethyl acetate). The combined organic extracts were washed with brine and dried over anhydrous sodium sulfate prior to filtration and evaporation of the solvent under reduced pressure.

Flash chromatography was performed on commercially available silica gel (0.035–0.070 nm pore diameter) and mixtures of freshly distilled petroleum ether 40–60 and ethyl acetate or reversed-phase silica gel (0.04–0.06 nm pore diameter Screening Devices) with freshly distilled mixtures of acetonitrile and ethyl acetate. Final purification was performed on Shimadzu preparative HPLC by using a C18 column (Alltech Alltima 250 mm × 22 mm; 5μ) with HPLC-grade water, acetonitrile, and ethyl acetate mixture.

Nuclear magnetic resonance spectroscopy and mass spectrometry: ^{1}H NMR and ^{13}C NMR spectra were determined on a Bruker CXP 300 NMR spectrometer in $CDCl_3$ solutions unless indicated otherwise. Chemical shifts are reported in ppm downfield relative to tetramethylsilane ($\delta = 0$ ppm for ^{1}H) or based on the solvent peak ($CDCl_3$) ($\delta = 77.00$ ppm for ^{13}C NMR) as an internal standard. HRMS was performed on a Finnigan Mat95 mass spectrometer.

Steady-state absorption and fluorescence: Absorption spectra of the oligodiacetylenes in *n*-hexane (spectrophotometric grade, Riedel-de Haën) and DCE (spectrophotometric grade, Sigma-Aldrich) were recorded by using a Cary 100 UV/Vis spectrophotometer (scan range: 200–800 nm, scan rate: 300 nm min^{-1}, date interval 0.5 nm) and steady-state fluorescence by using a FLS920P Spectrometer (slit exc.: 2 nm, slit em.: 2 nm, step: 1.0, dwell: 0.2 s). Absorption spectra of oligodiacetylenes in a film obtained by drop casting were recorded on a Cary 50 UV/Vis spectrophotometer (scan range 200–800 nm, scan rate 300 nm min^{-1}, data interval 0.5 nm).

Determination of fluorescence quantum yield in solution: To evaluate the fluorescence quantum yield (Φ_F) of an ODA solution in *n*-hexane or DCE, the areas of the corrected emission spectra were compared to a spectrum of a reference solution of quinine bisulfate in 0.1 M H_2SO_4 measured at 366 nm having $\Phi_F = 0.535$.[69] The fluorescence quantum yields of the ODAs were determined by the relationship:

$$\Phi_F = \Phi_R \frac{I}{I_R} \frac{OD_R}{OD} \frac{n^2}{n_R{}^2} \quad (4)$$

In which I and I_R are the integrated emission intensities of the ODA and quinine bisulfate solutions, respectively, OD refers to the optical densities of the respective solutions and n is the refractive index.

Lifetime of fluorescence and fluorescence anisotropy in solution: The fluorescence lifetime and anisotropy were recorded by using a FLS920P Spectrometer (Edinburgh Instruments) for time-correlated photon counting (TCSP) (time set up: 5 or 10 ns, 4096 channels; measurements stopped after 10000 counts were obtained, and for **1-*8*** in a separate experiment also after 24 h of data collection to check the influence of photochemistry occurring after prolonged irradiation). Pulsed diode lasers (372 nm, FWHM: 54 ps; 444 nm, FWHM: 63 ps) and pulsed LEDs (283 nm, FWHM $<$ 500 ps; 304 nm, FWHM: $<$ 350 ps (FWHM = full width at half-maximum)) from PicoQuant were used as light sources. The anisotropy measurements were performed by using vertical and horizontal polarizations. All spectroscopic measurements were carried out under magic angle conditions to avoid the possible influence of rotational motions of the probe molecules.

((*E*)-4-Iodo-3-propyloct-3-en-1-ynyl)trimethylsilane (2): A brown, 500 mL, two-necked, round-bottomed flask containing a solution of (*E*)-5-(trimethylsilyl)-4-(2-(trimethylsilyl)ethynyl)non-4-ene (**8**) (12.50 g, 42.5 mmol) and *N*-iodosuccinimide (20.0 g, 88.9 mmol) in CH_2Cl_2 (250 mL, distilled and degassed) was vigorously stirred for 3 h at room temperature under an argon atmosphere. After addition of a saturated aqueous solution of $Na_2S_2O_3$, the reaction mixture was worked up according to the general procedure and purified on reversed-phase silica (CH_3CN) to give a crude oil which was purified by reversed-phase chromatography (CH_3CN/H_2O, 90:10) to afford pure **2** (11.09 g, 31.9 mmol, 75%) as a colorless oil: ^{1}H NMR (300 MHz, $CDCl_3$): $\delta = 0.20$ (s, 9H), 0.95 (t, $J = 7.5$ Hz, 3H), 0.96 (t, $J = 7.7$ Hz, 3H), 1.35 (t, $J = 7.4$ Hz, 2H), 1.49–1.63 (m, 4H), 2.30 (t, $J = 7.7$ Hz, 3H), 2.88 ppm (t, $J = 7.4$ Hz, 3H); ^{13}C NMR: $\delta = 0.0$, 13.7, 14.1, 21.2, 21.5, 31.4, 43.3, 43.6, 99.4, 101.7, 119.2, 128.1 ppm; HRMS: *m*/*z* calcd 348.0770 found 348.0771;.

(*Z*)-3-(Iodo(trimethylsilyl)methylene)-1-(trimethylsilyl)hex-1-yne (7): A brown, 2 L, two-necked, round-bottomed flask filled with diethyl ether (1200 mL, dry and degassed) and equipped with four pressure-equalized dropping funnels containing **4** (15.00 g, 106.9 mmol, 19.6 mL), Ti(O*i*Pr)$_4$ (39.51 g, 139,0 mmol, 41.0 mL), a solution of *i*PrMgCl in diethyl ether (133.6 mL, 2.0 M, 267.3 mmol), and **3** (7.35 g, 74.8 mmol, 10.6 mL) was flushed with a constant flow of argon, stirred, and slowly cooled down to −78 °C. At −78 °C, **4** and Ti(O*i*Pr)$_4$ were added dropwise along with the 2.0 M solution of *i*PrMgCl. The solution was warmed up to −50 °C over 60 min and its color changed from pale yellow to brown. After the solution was stirred at −55 °C for 2 h, ethynyltrimethylsilane was added dropwise and the solution was stirred at −50 °C for a further 2 h. Iodine (62.4 g, 245.9 mmol) was added as a powder at −60 °C and then the mixture was slowly warmed up to room temperature and stirred for 2 h. The resulting mixture was filtered through a pad of Celite and washed with sodium thiosulfate solution and worked up according to the general procedure to give a crude oil of **6**, which was subjected to the elimination reaction. The crude oil was stirred at 0 °C in pyrrolidine (100 mL) during 1 h in a brown three-necked flask under an argon atmosphere. After dilution of the mixture with petroleum ether 40–60 (100 mL), ammonium chloride was added at 0 °C. The reaction mixture was worked up according to the general procedure, pre-purified on a silica gel column (5% Et_3N solution in petroleum ether 40–60) and finally purified on reversed-phase silica (CH_3CN/H_2O, 80:20) to give pure **7** (16.45 g, 45.21 mmol, 60%) as a colorless oil; ^{1}H NMR (300 MHz, $CDCl_3$): $\delta = 0.24$ (s, 9H), 0.31 (s, 9H), 0.93 (t, $J = 7.4$ Hz, 3H), 1.54–1.69 (m, 2H), 2.29–2.34 ppm (m, 2H); ^{13}C NMR (75 MHz, $CDCl_3$): $\delta = 0.0$, 2.1, 13.7, 22.7, 39.2, 99.9, 109.6, 117.3, 142.1 ppm; HRMS: *m*/*z* calcd 364.0540 observed 364.0539.

(*E*)-5-(Trimethylsilyl)-4-(2-(trimethylsilyl)ethynyl)non-4-ene (8): A brown, 1 L, three-necked, round-bottomed flask filled with **7** (16.45 g, 45.2 mmol) in THF (500 mL, dry and degassed) was equipped with two pressure-equalized dropping funnels filled with 1.6 M *n*BuLi solution in hexane (57 mL, 91 mmol) and 1-iodobutane (8.89 g, 48.3 mmol, 5.5 mL). The apparatus was kept under a continuous flow of argon. The solution was stirred vigorously at −78 °C and *n*BuLi was added dropwise over 60 min. After an additional 30 min, the 1-iodobutane was added to complete the reaction. The mixture was warmed up to room temperature, quenched with a saturated solution of NH_4Cl at 0 °C, and worked up according to the general procedure. The residue was purified on reversed-phase silica (CH_3CN) to give pure **8** (12.71 g, 43.2 mmol, 96%) as a colorless oil; ^{1}H NMR (300 MHz, $CDCl_3$): $\delta = 0.24$ (s, 9H), 0.31 (s, 9H), 0.92 (t, $J = 7.4$ Hz, 3H), 0.93 (t, $J = 7.4$ Hz, 3H), 1.35 (t, $J = 7.3$ Hz, 2H), 1.49–1.63 (m, 4H), 2.34 (t, $J = 7.5$ Hz, 3H), 2.41 ppm (t, $J = 7.4$ Hz, 3H); ^{13}C NMR (75 MHz, $CDCl_3$): $\delta = 0.0$, 0.3, 13.6, 14.0, 21.3, 21.5, 31.1, 43.5, 43.6, 99.4, 101.7, 119.2, 129.6 ppm; HRMS: calcd 294.2200; found 294.2199.

(*E*)-5-(Trimethylsilyl)-4-(2-(trimethylsilyl)ethynyl)dodec-4-ene (8a): A few drops of 1-bromoheptane (1.00 g, 5.58 mmol, 1.14 mL) were added to a stirred suspension of lithium (6.94 g, 100 mmol) in dry and degassed diethyl ether (50 mL) at room temperature under an argon atmosphere until the reaction mixture became cloudy. Then, the reaction mixture was cooled to −20 °C and the remaining 1-bromoheptane (16.91 g, 94.4 mmol, 14.8 mL) was added dropwise. This mixture was allowed to warm to room temperature and was stirred for 1 h. The solution was stored under argon and used without further purification. A brown 50 mL, three-necked, round-bottomed flask filled with **7** (450 mg, 1.24 mmol) in THF (25 mL, dry and degassed) was equipped with two pressure-equalized dropping funnels filled with ≈2.0 M *n*-HepLi solution in ether (5 mL, 2.5 mmol) and 1-bromoheptane (223.9 mg, 1.25 mmol, 0.20 mL). The apparatus was kept under a continuous flow of argon. The solution was stirred vigorously at −78 °C and *n*-HepLi was added dropwise over 30 min. After an additional 30 min, 1-bromoheptane was added to complete the reaction. The mixture was warmed up to room temperature, quenched with a saturated solution of NH_4Cl at 0 °C, and worked up according to the general procedure. The residue was purified on reversed-

phase silica (CH_3CN) to give **8a** (381 mg, 1.10 mmol, 88%) as a colorless oil. ^{1}H NMR (300 MHz, $CDCl_3$): δ=0.24 (s, 9H), 0.31 (s, 9H), 0.91 (t, J=7.4 Hz, 3H), 0.92 (t, J=7.4 Hz, 3H), 1.35 (t, J=7.3 Hz, 2H), 1.48–1.64 (m, 10H), 2.34 (t, J=7.5 Hz, 3H), 2.41 ppm (t, J=7.4 Hz, 3H); ^{13}C NMR: δ=0.0, 0.4, 13.4, 14.1, 21.3, 21.50, 31.1, 33.4, 34.2, 34.5, 43.4, 43.5, 99.3, 101.6, 119.0, 129.4 ppm; HRMS m/z: calcd: 336.2669 observed 336.2666.

(*E*)-5-Butyl-2-methyl-6-(2-(trimethylsilyl)ethynyl)non-5-en-3-yn-2-ol (9): A mixture of **2** (10.0 g, 28.7 mmol), 2-methylbut-3-yn-2-ol (4.83 g, 57.7 mmol, 5.6 mL), [Pd(PPh_3)$_4$] (1.62 g, 1.4 mmol), CuI (133 mg, 0.7 mmol), and dry, degassed diethylamine (70 mL) in THF (180 mL) was placed anaerobically in a dried 500 mL two-necked round-bottomed flask, equipped with a magnetic stirrer, an argon in- and outlet, and a pressure-equalized dropping funnel. The mixture was stirred for 4 h at 30°C, concentrated, and filtered over a short silica gel column (5% Et_3N solution in petroleum ether 40–60). The residue was purified on reversed-phase silica (CH_3CN/EtOAc 8.5:1.5) to give pure **9** (6.98 g, 23.0 mmol, 80%) as a pale yellow oil: ^{1}H NMR (300 MHz, $CDCl_3$): δ=0.20 (s, 9H), 0.92 (t, J=7.4 Hz, 3H), 0.93 (t, J=7.4 Hz, 3H), 1.35 (t, J=7.3 Hz, 2H), 1.49 (s, 6H), 1.49–1.63 (m, 4H), 2.35 (t, J=7.5 Hz, 3H), 2.42 ppm (t, J=7.4 Hz, 3H); ^{13}C NMR: δ=0.0, 13.6, 13.9, 21.6, 22.0, 31.5, 32.4, 34.6, 36.8, 68.7, 81.6, 101.3, 102.8, 104.4, 129.0, 130.7 ppm; HRMS: calcd 304.2222; found 304.2235.

((*E*)-4-Butyl-7-methoxy-7-methyl-3-propylocta-3-en-1,5-diynyl)trimethylsilane (1-*1*): A solution of **9** (6.50 g, 21.4 mmol) in dry, degassed THF (125 mL) was placed anaerobically in a dried 250 mL two-necked round-bottomed flask, equipped with a magnetic stirrer and an argon in-and outlet. Sodium hydride (1.0 g, 25.0 mmol, 60% dispersion in mineral oil) was added in small portions. After hydrogen evolution had ceased, MeI (4.26 g, 30 mmol, 1.87 mL) was added slowly and the mixture was warmed gently. After about 30 min NaI precipitated from the solution. The reaction was then quenched with H_2O (30 mL), and petroleum ether 40–60 (75 mL) was added followed by workup according to the general procedure. After purification on reversed-phase silica (CH_3CN/EtOAc 8.0:2.0) pure **1-*1*** (6.24 g, 19.6 mmol, 92%) was obtained as a pale yellow oil: ^{1}H NMR (300 MHz, $CDCl_3$): δ=0.20 (s, 9H), 0.92 (t, J=7.4 Hz, 3H), 0.93 (t, J=7.4 Hz, 3H), 1.35 (t, J=7.3 Hz, 2H), 1.49 (s, 6H), 1.49–1.63 (m, 4H), 2.35 (t, J=7.5 Hz, 3H), 2.42 (t, J=7.4 Hz, 3H), 3.37 ppm (s, 3H); ^{13}C NMR (75 MHz, $CDCl_3$): δ=0.0, 13.6, 13.9, 21.6, 22.0, 28.4, 30.4, 34.6, 36.8, 51.7, 71.2, 83.6, 100.3, 103.1, 104.4, 129.1, 130.5 ppm; HRMS: calcd: 318.2379; found: 318.2381.

General method for protodesilylation of oligodiacetylene series (1-*n*) followed by catalytic Sonogashira coupling with iododiacetylene (2) illustrated in Scheme 5: i) A solution of (**1-*n***) (1 equiv) in THF/MeOH (1:1, 5 mL/mmol) was stirred in a round-bottomed flask. H_2O (3 drops/mmol) and K_2CO_3 (2 equiv) were added to the solution and it was stirred for 3 h. After following the general workup procedure, the terminal acetylene (**10-*n***) was submitted to the catalytic chain elongation step (ii). ii) A mixture of **2** (10 equiv), [Pd(PPh_3)$_4$] (5 mol%), CuI (2 mol%), and dry, degassed diethylamine (2 mL/mmol) and THF (5 mL/mmol) was placed anaerobically in a dried, brown two-necked round-bottomed flask, equipped with a magnetic stirrer, an argon/hydrogen in- and outlet, and a pressure-equalized dropping funnel containing terminal acetylene (**10-*n***) (1 equiv). The terminal acetylene was added slowly (over 6 h) to the stirred mixture under a constant flow of argon/hydrogen (1:1). The mixture was further stirred overnight at 25°C, concentrated, and filtered over a short silica gel column (5% Et_3N solution in petroleum ether 40–60). The residue was pre-purified on reversed-phase silica (CH_3CN/EtOAc) and finally purified on preparative HPLC to give pure (99.5%) diacetylene (**1-*n***) and a quantitive recovery of iododiacetylene (**2**).

((3*E*,7*E*)-4,8-Dibutyl-11-methoxy-11-methyl-3,7-dipropyldodeca-3,7-dien-1,5,9-triynyl) trimethyl- silane (1-*2*): Pale yellow oil (2.22 g, 4.76 mmol, 82%) from **1-*1*** (1.85 g, 5.81 mmol); ^{1}H NMR (300 MHz, $CDCl_3$): δ=0.20 (s, 9H), 0.89–0.95 (m, 12H), 1.28–1.41 (m, 4H), 1.46 (s, 6H), 1.46–1.62 (m, 8H), 2.32–2.49 (m, 6H), 3.38 ppm (s, 3H); ^{13}C NMR (75 MHz, $CDCl_3$): δ=0.0, 13.6, 13.6, 13.9, 14.0, 21.7, 22.1, 22.2, 28.4, 30.5, 30.7, 34.7, 34.9, 36.9, 37.1, 51.7, 71.2, 84.0, 97.9, 98.5, 100.2, 103.7, 104.8, 128.8, 128.9, 129.4, 131.2 ppm; HRMS m/z: calcd: 466.3631; found 466.3634.

(3*E*,7*E*,11*E*)-4,8,12-Tributyl-15-methoxy-15-methyl-3,7,11-tripropylhexadeca-3,7,11-trien-1,5,9,13-tetraynyl) trimethylsilane (1-*3*): Yellow oil (1.08 g, 1.76 mmol, 78%) from **1-*2*** (1.05 g, 2.25 mmol); ^{1}H NMR (300 MHz, $CDCl_3$): δ=0.21 (s, 9H), 0.90–0.96 (m, 18H), 1.30–1.42 (m, 6H), 1.51 (s, 6H), 1.51–1.66 (m, 12H), 2.36–2.50 (m, 12H), 3.39 ppm (s, 3H); ^{13}C NMR (75 MHz, $CDCl_3$): δ=0.0, 13.6, 13.6, 13.6, 13.9, 14.0, 14.0, 21.8, 21.9, 22.1, 22.2, 22.3, 28.4, 30.5, 30.7, 30.8, 34.7, 34.9, 35.0, 37.0, 37.1, 37.3, 51.7, 71.2, 84.0, 98.4, 98.6, 98.6, 99.0, 100.30, 103.8, 104.8, 128.8, 128.9, 129.1, 129.5, 129.7, 131.3 ppm; HRMS: m/z calcd: 614.4883; found: 614.4888.

(5*E*,9*E*,13*E*)-5,9,13-Tributyl-2-methyl-14-(2-(trimethylsilyl) ethynyl)-6,10-dipropylheptadeca-5,9,13-trien-3,7,11-triyn-2-ol (1-3 OH): Pale yellow solid (300 mg, 0.50 mmol, 80%). ^{1}H NMR (300 MHz, $CDCl_3$): δ=0.20 (s, 9H), 0.90–0.96 (m, 18H), 1.30–1.42 (m, 6H), 1.51 (s, 6H), 1.51–1.66 (m, 12H), 2.36–2.50 ppm (m, 12H); ^{13}C NMR (75 MHz, $CDCl_3$): δ=0.0, 13.6, 13.6, 13.6, 13.9, 14.0, 14.0, 21.8, 21.9, 22.1, 22.2, 22.3, 28.4, 30.5, 30.7, 30.8, 34.7, 34.9, 35.0, 37.0, 37.1, 37.3, 71.2, 84.0, 98.4, 98.6, 98.6, 99.1, 100.3, 103.8, 104.8, 128.8, 128.9, 129.1, 129.5, 129.7, 131.3 ppm; HRMS m/z: calcd: 600.4726; found: 600.4719.

((3*E*,7*E*,11*E*,15*E*)-4,8,12,16-Tetrabutyl-19-methoxy-19-methyl-3,7,11,15-tetrapropylicosa-3,7,11,15-tetraen-1,5,9,13,17-pentaynyl)trimethylsilane (1-*4*): Yellow solid (1.31 g, 1.72 mmol, 75%) from **1-*3*** (1.41 g, 2.29 mmol); ^{1}H NMR (300 MHz, $CDCl_3$): δ=0.21 (s, 9H), 0.91–0.97 (m, 24H), 1.30–1.42 (m, 8H), 1.51 (s, 6H), 1.51–1.67 (m, 16H), 2.36–2.52 (m, 16H), 3.39 ppm (s, 3H); ^{13}C NMR: δ=0.0, 13.6, 13.6, 13.7, 13.9, 14.0, 21.8, 21.9, 22.1, 22.2, 22.3, 28.4, 30.5, 30.7, 30.8, 34.7, 34.9, 35.1, 35.1, 37.0, 37.1, 37.3, 51.7, 71.2, 84.0, 98.5, 98.7, 98.8, 99.2, 100.3, 103.8, 104.8, 128.8, 128.9, 129.2, 129.5, 129.6, 129.7, 131.3 ppm; HRMS m/z: calcd: 762.6135; found: 762.6131.

((3*E*,7*E*,11*E*,15*E*,19*E*)-4,8,12,16,20-Pentabutyl-23-methoxy-23-methyl-3,7,11,15,19-pentapropyltetracosa-3,7,11,15,19-pentaen-1,5,9,13,17,21-hexaynyl)trimethylsilane (1-*5*): Yellow solid (0.82 g, 0.90 mmol, 70%) from **1-*4*** (0.98 g, 1.29 mmol); ^{1}H NMR (300 MHz, $CDCl_3$): δ=0.21 (s, 9H), 0.90–0.97 (m, 30H), 1.30–1.43 (m, 10H), 1.51 (s, 6H), 1.51–1.68 (m, 20H), 2.37–2.52 (m, 20H), 3.39 ppm (s, 3H); ^{13}C NMR (75 ppm, $CDCl_3$): δ=0.0, 13.6, 13.6, 13.7, 13.9, 14.0, 21.8, 21.9, 22.1, 22.2, 22.3, 28.4, 30.6, 30.7, 30.9, 34.8, 34.9, 35.1, 37.0, 37.1, 37.3, 51.7, 71.2, 84.0, 98.5, 98.7, 98.8, 99.2, 99.3, 99.3, 100.3, 103.8, 104.9, 128.8, 128.9, 129.2, 129.2, 129.5, 129.6, 129.7, 129.7, 131.3 ppm; HRMS m/z: calcd: 910.7387 found: 910.7406.

((3*E*,7*E*,11*E*,15*E*,19*E*,23*E*)-4,8,12,16,20,24-Hexabutyl-27-methoxy-27-methyl-3,7,11,15,19,23-hexapropyloctacosa-3,7,11,15,19,23-hexaen-1,5,9,13,17,21,25-heptaynyl)trimethylsilane (1-*6*): Yellow solid (450 mg, 0.42 mmol, 72%) from **1-*5*** (528 mg, 0.58 mmol); ^{1}H NMR: (300 MHz, $CDCl_3$): δ=0.21 (s, 9H), 0.91–0.98 (m, 36H), 1.30–1.43 (m, 12H), 1.51 (s, 6H), 1.51–1.68 (m, 24H), 2.37–2.53 (m, 24H), 3.39 ppm (s, 3H); ^{13}C NMR: δ=0.0, 13.6, 13.6, 13.9, 14.0, 21.8, 21.9, 21.9, 22.1, 22.2, 22.3, 28.4, 30.6, 30.7, 30.9, 30.9, 34.8, 34.9, 35.1, 37.0, 37.1, 37.3, 51.7, 71.2, 84.0, 98.5, 98.7, 98.8, 99.2, 99.3, 99.3, 99.4, 99.4, 100.4, 103.8, 104.7, 128.8, 128.9, 129.2, 129.3, 129.5, 129.6, 129.7, 129.7, 131.3 ppm; HRMS: calcd: 1058.8639; found: 1058.8632.

((3*E*,7*E*,11*E*,15*E*,19*E*,23*E*,27*E*)-4,8,12,16,20,24,28-Heptabutyl-31-methoxy-31-methyl-3,7,11,15,19,23,27-heptapropyldotriaconta-3,7,11,15,-19,23,27-heptaen-1,5,9,13,17,21,25,29-octaynyl)trimethylsilane (1-*7*): Yellow-orange solid (140 mg, 1.16 mmol, 68%) from **1-*6*** (180 mg, 1.70 mmol); ^{1}H NMR (300 MHz, $CDCl_3$): δ=0.21 (s, 9H), 0.91–0.98 (m, 42H), 1.30–1.44 (m, 14H), 1.51 (s, 6H), 1.51–1.68 (m, 28H), 2.37–2.53 (m, 28H), 3.39 ppm (s, 3H); ^{13}C NMR (75 MHz, $CDCl_3$): δ=0.0, 13.6, 13.6, 13.9, 14.0, 21.8, 21.9, 22.1, 22.2, 22.3, 28.4, 30.6, 30.7, 30.9, 30.9, 34.8, 34.9, 35.1, 37.0, 37.1, 37.3, 51.7, 71.2, 84.0, 98.5, 98.7, 98.8, 99.2, 99.3, 99.3, 99.4, 99.4, 99.5, 100.4, 103.9, 104.9, 128.8, 128.9, 129.2, 129.3, 129.5, 129.6, 129.7, 129.7, 131.3 ppm; HRMS: calcd: 1206.9891; found: 1206.9886.

((3*E*,7*E*,11*E*,15*E*,19*E*,23*E*,27*E*,31*E*)-4,8,12,16,20,24,28,32-Octabutyl-35-methoxy-35-methyl-3,7,11,15,19,23,27,31-octapropylhexatriaconta-3,7,11,15,19,23,27,31-octaen-1,5,9,13,17,21,25,29,33-nonaynyl)trimethylsilane (1-*8*): Orange solid (80 mg, 0.06 mmol, 69%) from **1-*7*** (109 mg, 0.09 mmol); ^{1}H NMR(300 MHz, $CDCl_3$): δ=0.21 (s, 9H), 0.91–0.98 (m, 48H), 1.30–1.44 (m, 16H), 1.51 (s, 6H), 1.51–1.69 (m, 32H), 2.37–2.53 (m, 32H), 3.39 ppm (s, 3H); ^{13}C NMR (75 MHz, $CDCl_3$): δ=0.0, 13.6,

13.6, 13.9, 14.0, 21.8, 21.9, 21.9, 22.1, 22.2, 22.3, 28.4, 30.6, 30.7, 30.9, 30.9, 34.8, 34.9, 35.1, 37.0, 37.1, 37.3, 51.7, 71.2, 84.0, 98.5, 98.7, 98.8, 99.2, 99.3, 99.3, 99.4, 99.4, 100.4, 103.9, 104.9, 128.8, 128.9, 129.2, 129.3, 129.5, 129.6, 129.7, 129.7, 131.3 ppm; HRMS *m*/*z*: calcd: 1355.1143; found: 1355.1156.

Acknowledgements

The authors thank the Dutch Technology Foundation STW for generous funding of this research (project no. WPC 5740), and Dr. J. Kroon (ECN), Dr. H. Schoo (TNO), Dr. J. Smits (Shell), and Prof. W. Jan Buma (University of Amsterdam) for helpful discussions.

[1] C. K. Chiang, C. R. J. Fincher, Y. W. Park, A. J. Heeger, H. Shirakawa, E. J. Louis, S. C. Gau, A. G. MacDiarmid, *Phys. Rev. Lett.* **1977**, *39*, 1098–1101.
[2] H. Shirakawa, E. J. Louis, A. G. MacDiarmid, C. K. Chiang, A. J. Heeger, *J. Chem. Soc. Chem. Commun.* **1977**, 578–580.
[3] R. H. Friend, R. W. Gymer, A. B. Holmes, J. H. Burroughes, R. N. Marks, C. Taliani, D. D. C. Bradley, D. A. Dos Santos, J. L. Bredas, M. Logdlund, W. R. Salaneck, *Nature* **1999**, *397*, 121–128.
[4] F. Diederich, *Chem. Commun.* **2001**, 219–227.
[5] M. B. Nielsen, F. Diederich, *Chem. Rev.* **2005**, *105*, 1837–1867.
[6] K. Kuriyama, H. Kikuchi, T. Kajiyama, *Langmuir* **1996**, *12*, 6468–6472.
[7] J. M. Tour, *Chem. Rev.* **1996**, *96*, 537–553.
[8] Q. Liu, W. Liu, B. Yao, H. Tian, Z. Xie, Y. Geng, F. Wang, *Macromolecules* **2007**, *40*, 1851–1857.
[9] P. Frere, J.-M. Raimundo, P. Blanchard, J. Delaunay, P. Richomme, J.-L. Sauvajol, J. Orduna, J. Garin, J. Roncali, *J. Org. Chem.* **2003**, *68*, 7254–7265.
[10] M. R. Bryce, M. A. Coffin, P. J. Skabara, A. J. Moore, A. S. Batsanov, J. A. K. Howard, *Chem. Eur. J.* **2000**, *6*, 1955–1962.
[11] C. Czekelius, J. Hafer, Z. J. Tonzetich, R. R. Schrock, R. L. Christensen, P. Mueller, *J. Am. Chem. Soc.* **2006**, *128*, 16664–16675.
[12] G. Zotti, G. Schiavon, A. Berlin, G. Pagani, *Chem. Mater.* **1993**, *5*, 430–436.
[13] G. Zotti, G. Schiavon, A. Berlin, G. Pagani, *Chem. Mater.* **1993**, *5*, 620–624.
[14] G. Zotti, G. Schiavon, A. Berlin, G. Pagani, *Adv. Mater.* **1993**, *5*, 551–554.
[15] W. Ten Hoeve, H. Wynberg, E. E. Havinga, E. W. Meijer, *J. Am. Chem. Soc.* **1991**, *113*, 5887–5889.
[16] S. S. Zade, M. Bendikov, *J. Org. Chem.* **2006**, *71*, 2972–2981.
[17] D. Fichou, G. Horowitz, B. Xu, F. Garnier, *Synth. Met.* **1990**, *39*, 243–259.
[18] U. Segelbacher, N. S. Sariciftci, A. Grupp, P. Baeuerle, M. Mehring, *Synth. Met.* **1993**, *57*, 4728–4733.
[19] J. Roncali, *Chem. Soc. Rev.* **2005**, *34*, 483–495.
[20] R. Sander, V. Stuempflen, J. H. Wendorff, A. Greiner, *Macromolecules* **1996**, *29*, 7705–7708.
[21] K. A. Walters, K. D. Ley, K. S. Schanze, *Langmuir* **1999**, *15*, 5676–5680.
[22] B. Leibrock, O. Vostrowsky, A. Hirsch, *Eur. J. Org. Chem.* **2001**, 4401–4409.
[23] J.-M. Kim, Y. B. Lee, D. H. Yang, J.-S. Lee, G. S. Lee, D. J. Ahn, *J. Am. Chem. Soc.* **2005**, *127*, 17580–17581.
[24] R. E. Martin, F. Diederich, *Angew. Chem.* **1999**, *111*, 1440–1469; *Angew. Chem. Int. Ed.* **1999**, *38*, 1351–1377.
[25] R. E. Martin, U. Gubler, J. Cornil, M. Balakina, C. Boudon, C. Bosshard, J.-P. Gisselbrecht, F. Diederich, P. Gunter, M. Gross, J.-L. Bredas, *Chem. Eur. J.* **2000**, *6*, 3622–3635.
[26] J. F. Nierengarten, D. Guillon, B. Heinrich, J. F. Nicoud, *Chem. Commun.* **1997**, 1233–1234.
[27] Y. Zhao, R. R. Tykwinski, *J. Am. Chem. Soc.* **1999**, *121*, 458–459.
[28] Y. Zhao, R. McDonald, R. R. Tykwinski, *J. Org. Chem.* **2002**, *67*, 2805–2812.
[29] S. C. Ciulei, R. R. Tykwinski, *Org. Lett.* **2000**, *2*, 3607–3610.
[30] Y. Zhao, S. C. Ciulei, R. R. Tykwinski, *Tetrahedron Lett.* **2001**, *42*, 7721–7723.
[31] H. Zuilhof, H. M. Barentsen, M. Dijk van, E. J. R. Sudhölter, R. J. O. M. Hoofman, L. D. A. Siebbeles, M. P. Haas de, J. M. Warman in *Polydiacetylenes*, (Ed. H. S. Nalwa), Academic Press, San Diego, **2001**, pp. 339–437.
[32] A. F. Garito, C. C. Teng, K. Y. Wong, O. Zammani′Khamiri, *Mol. Cryst. Liq. Cryst.* **1984**, *106*, 219–258.
[33] K. J. Donovan, E. G. Wilson, *Synth. Met.* **1989**, *28*, 569–574.
[34] S. Spagnoli, K. J. Donovan, K. Scott, M. Somerton, E. G. Wilson, *Chem. Phys.* **1999**, *250*, 71–79.
[35] V. Enkelmann, *Adv. Polym. Sci.* **1984**, *63*, 91–136.
[36] S. Jo, H. Yoshikawa, A. Fujii, M. Takenaga, *Synth. Met.* **2005**, *150*, 223–226.
[37] M. Schott, *Synth. Met.* **2003**, *139*, 739–742.
[38] F. Wudl, S. P. Bitler, *J. Am. Chem. Soc.* **1986**, *108*, 4685–4687.
[39] S. P. Bitler, F. Wudl, *Polym. Mater. Sci. Eng.* **1986**, *54*, 292–296.
[40] R. Giesa, R. C. Schulz, *Polym. Int.* **1994**, *33*, 43–60.
[41] D. J. Ager, *Synthesis* **1984**, 384–398.
[42] W. E. Lindsell, P. N. Preston, P. J. Tomb, *J. Organomet. Chem.* **1992**, *439*, 201–212.
[43] a) M. Polhuis, C. C. J. Hendrikx, H. Zuilhof, E. J. R. Sudhölter, *Tetrahedron Lett.* **2003**, *44*, 899–901; b) G. S. Pilzak, B. van Lagen, E. J. R. Sudhölter, H. Zuilhof, *Tetrahedron Lett*. **2008**, in press.
[44] C. C. J. Hendrikx, M. Polhuis, A. Pul-Hootsen, R. B. M. Koehorst, A. Hoek van, H. Zuilhof, E. J. R. Sudhölter, *Phys. Chem. Chem. Phys.* **2005**, *7*, 548–553.
[45] G. M. Balkowski, M. Groeneveld, H. Zhang, H. C. C. J. Hendrikx, M. Polhuis, H. Zuilhof, W. J. Buma, *J. Phys. Chem. A* **2006**, *110*, 11435–11439.
[46] Y. Takayama, C. Delas, K. Muraoka, F. Sato, *Org. Lett.* **2003**, *5*, 365–368.
[47] Y. Takayama, C. Delas, K. Muraoka, M. Uemura, F. Sato, *J. Am. Chem. Soc.* **2003**, *125*, 14163–14167.
[48] F. Sato, S. Okamoto, *Adv. Synth. Catal.* **2001**, *343*, 759–784.
[49] K. Fukuhara, Y. Takayama, F. Sato, *J. Am. Chem. Soc.* **2003**, *125*, 6884–6885.
[50] B. J. Wakefield, *The Chemistry Of Organolithium Compounds*, Pergamon Press Ltd., **1974**.
[51] Alkylation of diacetylene **7** followed by GC/MS. Use of *t*BuLi and *n*BuI resulted in formation of **8** along with the protonated analogue in a ratio of 80:20. Use of *n*BuLi with *n*-propyllithium resulted in formation of **8** along with its analogue bearing two propyl side chains in a ratio of 60:40 as determined by GC/MS.
[52] V. A. Solomin, W. Heitz, *Macromol. Chem. Phys.* **1994**, *195*, 303–314.
[53] G. S. Pilzak, S. Fratiloiu, F. Grozema, L. D. A. Siebbeles, H. Zuilhof, unpublished results.
[54] P. Siemsen, R. C. Livingston, F. Diederich, *Angew. Chem.* **2000**, *112*, 2740–2767; *Angew. Chem. Int. Ed.* **2000**, *39*, 2632–2657.
[55] A. Elangovan, Y.-H. Wang, T.-I. Ho, *Org. Lett.* **2003**, *5*, 1841–1844.
[56] S. Urgaonkar, J. G. Verkade, *J. Org. Chem.* **2004**, *69*, 5752–5755.
[57] B. E. Kohler, D. E. Schilke, *J. Chem. Phys.* **1987**, *86*, 5214–5215.
[58] Y. Zhao, K. Campbell, R. R. Tykwinski, *J. Org. Chem.* **2002**, *67*, 336–344.
[59] S. M. Bachilo, E. V. Bachilo, T. Gillbro, *Chem. Phys.* **1998**, *229*, 75–91.
[60] J. Gierschner, J. Cornil, H. Egelhaaf, *J. Adv. Mater.* **2007**, 173–191.
[61] S. S. Zade, M. Bendikov, *Org. Lett.* **2006**, *8*, 5243–5246.
[62] G. Wenz, M. A. Müller, M. Schmidt, G. Wegner, *Macromolecules* **1984**, *17*, 837–850.
[63] R. E. Martin, U. Gubler, J. Cornil, M. Balakina, C. Boudon, C. Bosshard, J.-P. Gisselbrecht, F. Diederich, P. Günter, M. Gross, J.-L. Brédas, *Chem. Eur. J.* **2000**, *6*, 3622–3635.
[64] R. Lecuiller, J. Berrehar, C. Lapersonne-Meyer, M. Schott, *Phys. Rev. Lett.* **1998**, *80*, 4068–4071.

[65] B. E. Kohler, D. E. Schilke, *J. Chem. Phys.* **1987**, *86*, 5214–5215.
[66] M. Yoshizawa, A. Kubo, S. Saikan, *Phys. Rev. B* **1999**, *60*, 15632–15635.
[67] T. Itoh, B. E. Kohler, C. W. Spangler, *Spectrochim. Acta* **1994**, *50 A*, 2261–2263.
[68] S. M. Bachilo, C. W. Spangler, T. Gillbro, *Chem. Phys. Lett.* **1998**, *283*, 235–242.
[69] J. R. Lakowicz in *Principles of Fluorescence Spectroscopy*, Kluwer Academic/Plenum Publishers, **1999**, pp. 420–421.
[70] P. Kapusta, R. Erdmann, U. Ortmann, M. Wahl, *J. Fluoresc.* **2003**, *13*, 179–183.
[71] I. Soutar, L. Swanson, *Polym. Int.* **2006**, *55*, 729–739.
[72] X. Dou, Q. Y. Shang, B. S. Hudson, *Chem. Phys. Lett.* **1992**, *189*, 48–53.
[73] N. Aratani, Z. S. Yoon, D. Kim, A. Osuka, *J. Chin. Chem. Soc.* **2006**, *53*, 41–46.

Received: February 7, 2008
Published online: July 9, 2008

